J. Fluid Mech. (1991), *vol.* 226, *pp.* 497–509
Printed in Great Britain

Mach reflection of a ring shock wave from the axis of symmetry

By E. M. BARKHUDAROV, M. O. MDIVNISHVILI, I. V. SOKOLOV†, M. I. TAKTAKISHVILI AND V. E. TEREKHIN

†General Physics Institute, Vavilova 38, 117942 Moscow, USSR

(Received 25 October 1989 and in revised form 30 July 1990)

The paper is devoted to the theoretical and experimental investigation of the ring (toroidal) shock wave near the axis of symmetry. The theoretical approach is based upon the Chester–Chisnell–Whitman method. The experimental toroidal shock wave is generated by a novel inducer and visualized by the shadow technique. Attention is paid to the manner of reflection of the shock wave from the axis of symmetry. This reflection appears to be irregular even at small distances from the centre of the ring. This phenomenon is due to the cumulative acceleration of the converging axisymmetric shock front near the axis. The acceleration results in an increase in the incidence angle up to that characteristic of Mach (irregular) reflection.

1. Introduction

The convergence of one-dimensional spherical or cylindrical shock waves is known to be accompanied by an unlimited increase in energy density as the shock front approaches the centre (axis) of symmetry – unlimited amplification (Guderley 1942; Stanyukowich 1955).

The present paper is devoted to a more general case – an axisymmetric non-one-dimensional shock wave, converging to the axis. The most typical example is a ring shock wave. Let us suppose that a thin round ring (torus) explodes in a perfect gas, resulting in ring (toroidal) shock wave generation (figure 1). We shall now study some details of the corresponding flow both, experimentally and theoretically.

As the ring shock front approaches the centre of the ring, the wave amplitude, characterized by the front velocity V, increases, the increase being unlimited. This has been shown both experimentally (Berejetskaya *et al.* 1984) and theoretically (Sokolov 1986). The conclusion on unlimited amplification of the ring shock front is not obvious, because in non-one-dimensional flow the energy can flow out from the centre in opposite directions along the axis (see figure 1), and this process tends to limit the amplification.

In the present paper we study some details of the flow pattern after the shock wave comes to the centre. It is shown that the axisymmetric shock front is reflected from the axis of symmetry in the Mach manner, such reflection being predicted and observed at small (perhaps infinitesimal) distances from the ring centre.

This conclusion is in full agreement with the well-known hypothesis (Courant & Friedrichs, 1948) that the axisymmetric ('conical') convergent shock wave undergoes Mach reflection in every case, in contrast to a planar shock, which can also be reflected in a regular manner.

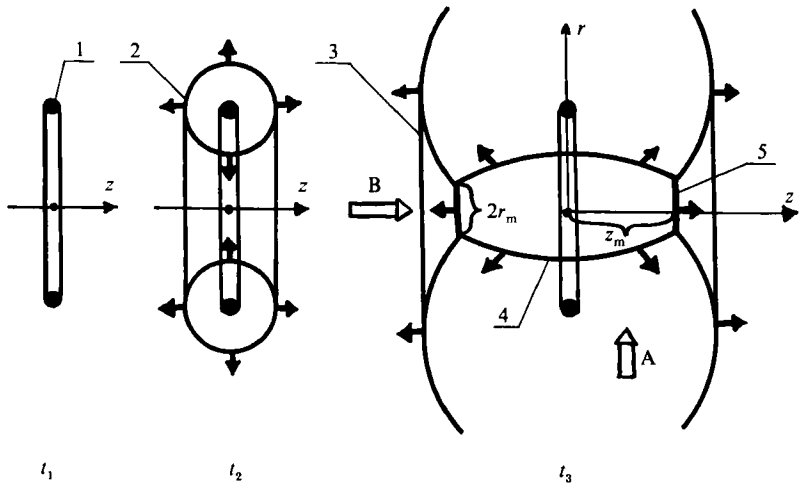

FIGURE 1. Ring (toroidal) shock wave at successive times $t_1 > t_2 > t_3$: curve 1, energy release region; 2, ring shock front before the moment of cumulation; 3, ring shock front after the cumulation; 4, the part of the ring shock 3 reflected from the axis; 5, Mach shock wave. The shadow photographs are taken along the direction of either arrow A or B.

2. The theory

The main characteristic features of shock front behaviour when the ring wave converges to the axis may be easily revealed by means of shock wave dynamics – the Chester–Chisnell–Whitham method (Whitham 1974). According to this approximate theory the shock front positions at successive times t are described by the equation

$$\Phi(r, z, \varphi) + V_{so}\, t = 0, \tag{2.1}$$

r, z, φ being the coordinates of any point belonging to a mathematical surface which coincides with the shock wave front. Here we use cylindrical coordinates, and V_{so} is the sound speed in the uniform gas before the front. Whitham obtained the approximate equations for the function Φ:

$$\nabla \cdot (M^{n+1} \nabla \Phi) = 0, \tag{2.2}$$

$$M = |\nabla \Phi|^{-1}, \tag{2.3}$$

M being the local Mach number of the shock front and n being a constant which depends only upon the polytropic index γ:

$$n = 1 + 2/\gamma + [2\gamma/(\gamma - 1)]^{\frac{1}{2}} \approx 5.1 \quad \text{for} \quad \gamma = \tfrac{7}{5}. \tag{2.4}$$

Equation (2.2) is the strong shock approximation ($M \to \infty$) of shock wave dynamics.

In the case of axisymmetric motion, (2.2) and (2.3) give:

$$\frac{1}{r}\frac{\partial}{\partial r}\left(M^{n+1} r \frac{\partial \Phi}{\partial r}\right) + \frac{\partial}{\partial z}\left(M^{n+1} \frac{\partial \Phi}{\partial z}\right) = 0, \tag{2.5}$$

$$M = \left[\left(\frac{\partial \Phi}{\partial r}\right)^2 + \left(\frac{\partial \Phi}{\partial z}\right)^2\right]^{-\frac{1}{2}}. \tag{2.6}$$

Equations (2.5) and (2.6) have a solution

$$\Phi_0 = C_0 r^{(n+1)/n}, \tag{2.7}$$

$$M = \frac{n}{(n+1)C_0} r^{-1/n}, \tag{2.8}$$

C_0 being an arbitrary positive constant. These formulae describe the cylindrical (independent of z) converging shock wave. The relation (2.8) is in excellent agreement with the self-similar solution of Guderley–Landau–Stanyukowich (Whitham 1974).

Now we apply the Chester–Chisnell–Whitham method (CCW) to investigate the axisymmetric converging shock wave (depending on z as well as r). This type of symmetry is more general than the cylindrical one. Nevertheless, it may be assumed that the CCW method supplies a good approximation in the neighbourhood of the axis.

In the vicinity of a point 0 on the axis we can obtain a solution of (2.5) and (2.6) in the form of a local expansion in a power series in r, z, the first term being equal to (2.7):

$$\Phi = \Phi_0 + \Phi_1, \tag{2.9}$$

$$\Phi_1 = \sum_{p,q} a_{pq} r^p z^q, \quad a_{pq} = \text{const.} \tag{2.10}$$

If the sum $s = p+q$ for all the terms in Φ_1 is higher than the degree of Φ_0 ($s > 1+1/n$), we can find Φ_1 as a linear correction to Φ_0. In our case the expansion (2.9) gives an asymptotic approximation for $\nabla\Phi$, as long as r and z satisfy the condition

$$\Phi(r,z) \geqslant 0. \tag{2.11}$$

This means that, when r and z tend to zero along any curve $r(z)$ and r and z satisfy (2.11), the expansion (2.9) gives the asymptotic approximation for $\nabla\Phi$ with respect to the parameter $R = (r^2+z^2)^{\frac{1}{2}} \to 0$.

The physical meaning of (2.11) is evident: we can apply the expansion (2.9) for the shock wave front description only before time $t = 0$, when it reaches the axis. The condition $t \leqslant 0$ along with (2.1) results in (2.11).

It will be shown below that after the instant $t = 0$ the shock wave reflection from the axis results in a rather complicated form of the wave front, including triple shock configurations. That is why (2.9) is invalid for some r and z belonging to the region where $\Phi(r,z) \geqslant 0$. On the other hand, it will be shown that the condition for the validity of (2.9) is actually weaker than (2.11).

The asymptotic approximate equation for the linear correction Φ_1 may be obtained when the conditions

$$|\partial\Phi_1/\partial r| \ll |\partial\Phi_0/\partial r|, \tag{2.12}$$

$$|\partial\Phi_1/\partial z| \ll |\partial\Phi_0/\partial r|, \tag{2.13}$$

are fulfilled. In this case the terms in (2.5) may be expressed as follows:

$$\frac{\partial}{\partial z}\left(M^{n+1}\frac{\partial\Phi}{\partial z}\right) \approx \frac{\partial^2\Phi_1}{\partial z^2}\left(\frac{\partial\Phi_0}{\partial r}\right)^{-(n+1)}, \tag{2.14}$$

because $\partial\Phi_0/\partial z \equiv 0$, and

$$\frac{1}{r}\frac{\partial}{\partial r}\left(rM^{n+1}\frac{\partial\Phi}{\partial r}\right) \approx -\frac{n}{r}\frac{\partial}{\partial r}\left(r\frac{\partial\Phi_1/\partial r}{(\partial\Phi_0/\partial r)^{n+1}}\right), \tag{2.15}$$

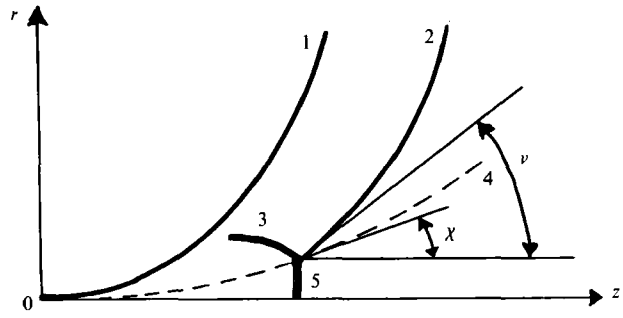

FIGURE 2. The flow pattern in the neighbourhood of the axis and the regions of applicability of different expansions ($t \geqslant 0$). Curve 1, incident shock wave at $t = 0$; 2, incident shock wave at $t > 0$; 3, reflected shock wave; 4, trajectory of the triple point; 5, Mach wave. The outer expansion is applicable in the region above curve 4. The inner expansion is applicable below curve 1. The inner expansion is matched with the Mach wave on line 4.

because $(\partial/\partial r)\,(r\,(\partial\Phi_0/\partial r)^{-n}) \equiv 0$. The conditions (2.12) and (2.13) are used for the linearization of M. So the equation for Φ_1 becomes

$$\frac{\partial^2\Phi_1}{\partial z^2} = nr^{1/n}\frac{\partial}{\partial r}\left(r^{-1/n}\frac{\partial\Phi_1}{\partial r}\right). \tag{2.16}$$

The first two terms of the expansion (2.10) for the solution of (2.16) may be represented as

$$\Phi_1 = -C_1[(n-1)z^2 + r^2], \quad C_1 = \text{const.} \tag{2.17}$$

Having introduced new constants R_0 and C instead of C_0 and C_1, we can rewrite (2.9), (2.7) and (2.17) in the form

$$\Phi = CR_0\left[\left(\frac{n}{n+1}\right)\left(\frac{r}{R_0}\right)^{(n+1)/n} - \frac{1}{2}\left(\frac{z}{R_0}\right)^2 - \frac{1}{2n-2}\left(\frac{r}{R_0}\right)^2\right], \tag{2.18}$$

the constant C being dimensionless and R_0 having the dimensions of length. The condition of applicability of the linearization procedure, which results in (2.18), may be easily obtained from (2.12), (2.13) and (2.18):

$$R_0 \gg R = (z^2 + r^2)^{\frac{1}{2}}, \tag{2.19}$$

$$r \gg r_1(z) = R_0(z/R_0)^n. \tag{2.20}$$

Once these conditions are satisfied, (2.18) permits us to describe the form of the shock front. It is drawn schematically in figure 2. Before time $t = 0$ the shock front does not intersect the axis and at $t = 0$ it touches the axis at the single point 0 ($r = 0$, $z = 0$). At that moment the shock front form is described by the equation

$$r = r_0(z) = R_0\left(\frac{n+1}{2n}\frac{z^2}{R_0^2}\right)^{n/(n+1)}. \tag{2.21}$$

We can see that the conditions (2.11) (i.e. $r \geqslant r_0(z)$) and (2.19) result in (2.20). It should be emphasized that the linearization is applicable even though on the curve (2.21) the first approximation is comparable with the linear correction ($\Phi_0 = -\Phi_1$). The point is that the conditions (2.19) and (2.20) restrict the values of the gradient of the linear correction rather than the value of the function itself.

The curve (2.21) has the form of a non-quadratic parabola $r \sim z^{\beta}$, $1 < \beta < 2$. It should be noted that the radius of curvature of this parabola equals zero at the point $r = 0$, $z = 0$. This results from the acceleration of the converging front due to amplification, because the point of the front that is nearest to the axis moves faster than the adjacent points. The influence of the cumulative acceleration upon the form of the converging front is also discussed below.

It is possible to obtain the dependence of the velocity of the converging front upon r in the plane of symmetry ($z = 0$). Equations (2.6) and (2.18) give (Sokolov 1986)

$$M \approx \left(\frac{r}{R}\right)^{-1/n}\left(1+\frac{1}{n-1}\left(\frac{r}{R}\right)^{1-1/n}\right). \tag{2.22}$$

The velocity increases beyond all bounds as the front converges to the axis, i.e. amplification is unlimited.

This general type of behaviour of an axisymmetric converging shock wave near the axis is obviously inherent to a ring shock wave near the centre of the ring. The free parameter C may be determined by comparison with the results of a numerical simulation of a ring shock wave (Kossyi *et al.* 1987) but here it is not essential. The constant R_0 is determined below by comparison of the theory with experimental data. It is evident in advance that R_0 is of the order of the ring radius R.

Let us proceed to the reflection of the shock front from the axis. On introducing an angle ν between the front and the axis into (2.5) and (2.6), it is easy to replace these by the system (Whitham 1974)

$$\frac{\partial}{\partial z}\left(\frac{\cos\nu}{M}\right)+\frac{\partial}{\partial r}\left(\frac{\sin\nu}{M}\right) = 0, \tag{2.23}$$

$$\frac{\partial}{\partial z}(M^n \sin\nu)-\frac{1}{r}\frac{\partial}{\partial r}(rM^n\cos\nu) = 0, \tag{2.24}$$

$$\frac{\partial \Phi}{\partial r} = \frac{\cos\nu}{M}, \quad \frac{\partial \Phi}{\partial z} = -\frac{\sin\nu}{M}. \tag{2.25}$$

These equations come from Whitham's equations (Whitham 1974, eq. 8.101). It should be emphasized that here we use the angle ν between the front and the axis rather than the angle θ between the axis and the normal to the front used by Whitham. Whitham's angle θ is negative in the problem involved, because the radial front velocity V_r is directed towards the axis and $\sin\theta = V_r/(MV_{so}) < 0$. From geometric considerations $\nu+(-\theta) = \frac{1}{2}\pi$.

To obtain a solution of (2.23)–(2.25) in the region

$$r \sim r_1(z) \tag{2.26}$$

where (2.20) is not satisfied and hence (2.18) is invalid, we can use the method of matched asymptotic expansions (Nayfeh 1981). The theory is valid provided $R/R_0 \to 0$. Outer expansion (2.18) is applicable through the condition (2.20). Now we can look for an inner expansion in the region (2.26) in the following form:

$$M = R_0 f(\lambda)/z, \quad \nu = \nu(\lambda), \quad \lambda = r/r_1(z). \tag{2.27}$$

For $\lambda \sim 1$ we have the estimate

$$\frac{\partial}{\partial z} \sim (z/R_0)^{n-1}\frac{\partial}{\partial r} \ll \frac{\partial}{\partial r},$$

so that (2.23), (2.24) and (2.27) give

$$\frac{\sin\nu}{f} = a_1, \quad \lambda f^n \cos\nu = a_2, \tag{2.28}$$

where a_1 and a_2 are constants. On estimating the terms that are neglected in (2.28), we can obtain the condition of applicability of inner expansion as

$$r \ll r_0(z). \tag{2.29}$$

The outer expansion is applicable in the region above curve 4 in figure 2 (see above). The inner one is valid below curve 1. The inner expansion is matched with a Mach wave on the line 4.

In the region $r_1 \ll r \ll r_0(z)$ both inner and outer expansions are applicable. In order to obtain expressions for the constants of the inner expansion we can compare (2.28) in case $\lambda \to \infty$ ($\nu \to 0$) with the expressions for M and ν ($\nu \to 0$) resulting from (2.18). Using (2.6) and the formula $\tan\nu = -(\partial\Phi/\partial z)/(\partial\Phi/\partial r)$, we obtain for the outer and inner expansions

$$M = ((\partial\Phi/\partial r)^2 + (\partial\Phi/\partial z)^2)^{-\frac{1}{2}} \approx C^{-1}(r/R_0)^{-1/n}, \quad M = a_2^{1/n}(r/R_0)^{-1/n}, \tag{2.30}$$

$$\nu \approx -\frac{\partial\Phi/\partial z}{\partial\Phi/\partial r} \underset{\text{(outer)}}{\approx} (z/R_0)(r/R_0)^{-1/n}, \quad \nu = a_1 a_2^{1/n}(z/R_0)(r/R_0)^{1/n}, \tag{2.31}$$

Hence $a_2 = C^{-n}$, $a_1 = C$.

It is easy to see that the acceleration of the converging shock wave is accompanied by an increase in the angle between the shock front and the axis. Once the cumulative acceleration is not limited (in the absence of dissipative effects), the increase in the angle is not limited either. But the reflection (or self-interaction) of the front with a rather high value of the angle of incidence cannot be regular, and there must be Mach reflection. That is why, just after the incident shock wave reaches the point 0, two Mach shock waves are formed at this point and move along the axis in opposite directions.

It should be emphasized that we use the CCW method only for describing the propagation of the incident shock wave, rather than the Mach reflection itself. In order to match the inner expansion with the Mach configuration and to obtain the characteristics of the configuration, for example the radius $r_m(z)$ of the Mach shock front, we need to know the relation between the angle of incidence ν_i at the triple point (figure 3) and the value of the angle

$$\chi = \arctan(\mathrm{d}r_m/\mathrm{d}z) \tag{2.32}$$

which characterizes the rate of growth of the Mach disk radius (figure 3). The relation

$$\chi = \chi(\nu_i), \tag{2.33}$$

along with (2.32) and the consequence from (2.28) that

$$\frac{r_m}{R_0} = \left(\frac{z}{R_0}\right)^n \frac{1}{(\sin\nu_i)^n \cos\nu_i}, \tag{2.34}$$

allow us to determine $r_m(z)$. We can take $\chi = 0$ as long as $\nu_i = \nu_{st}$, ν_{st} being the angle of incidence for stationary Mach reflection. The stationary Mach reflection is known

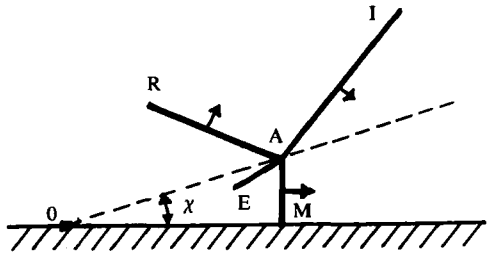

FIGURE 3. Mach reflection of a planar shock wave from a rigid plane. AI, incident ring shock wave; AR, reflected shock wave; AM, Mach shock; AE, contact surface; A0, trajectory of the triple point; χ, angle of motion of the triple point.

to be a particular case of Mach reflection of a shock front from a rigid plane, and is defined by the condition $\chi = 0$ (Courant & Friedrichs 1948). On substituting ν_i for ν_{st} in (2.34), we have

$$r_m = \frac{R_0}{\cos \nu_{st}} \left[\frac{z}{R_0 \sin \nu_{st}} \right]^n, \tag{2.35}$$

and in the vicinity of the point $r = 0$, $z = 0$, according to (2.32) and (2.35), $\chi \to 0$. This confirms the stationary character of the Mach reflection. When the Mach wave is not very close to the point $z = 0$, $r = 0$, the reflection is no longer stationary and we should use another relation (2.33).

The velocity V_m of the Mach shock wave may be obtained using (2.28) and the relation $V_m = V_i / \sin \nu_i$, where V_i is the velocity of the incident shock wave at the triple point:

$$V_m = \frac{V_{so} R_0}{Cz}. \tag{2.36}$$

Thus in the vicinity of 0 ($z/R_0 \to 0$), the Mach shock wave is of small size, but of high speed.

3. Experiment

The experimental ring shock wave is induced by means of the surface breakdown of numerous spark gaps arranged along the inner surface of a ring, facing the axis of symmetry. The general principle of the shock inducer is analogous to that described in Berejetskaya *et al.* (1984). But for the present study we have increased the number of sparks up to 100, and have arranged them more reasonably in order to achieve a more uniform energy release into the gas. As a result the inducer forms a practically homogeneous ring plasma filament. The energy release in the filament generates a ring (toroidal) shock wave in the gas.

The radius of the filament (R_r) is 5 cm, i.e. the total length of the filament, $\mathscr{L}$, is equal to approximately 32 cm. The experiments are performed in air at atmospheric pressure.

The energy release in the discharge is $\mathscr{E} \leqslant 1.2$ kJ. The duration of the discharge is about 30 μs. The average Mach number of the induced shock wave propagating toward the axis is about 2.

The shock wave is visualized by shadow photography, using a ruby laser as a source of light. The probing laser beam is directed at a right angle to the axis of the

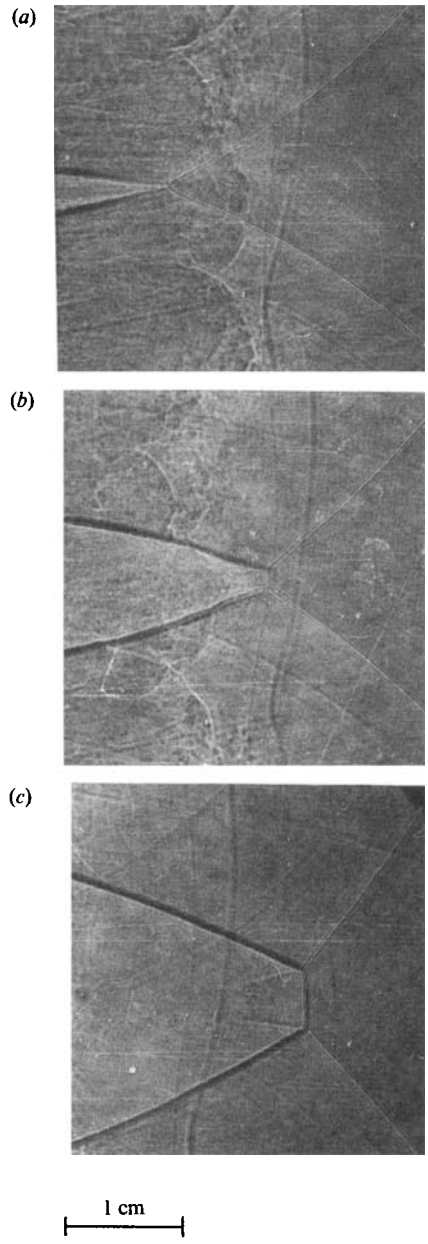

FIGURE 4. Shadow picture sequence. The inducer of the ring shock is on the left (*a*) time $t = 80$ μs, coordinate of Mach wave $z = 1.4$ cm; (*b*) $t = 87$ μs, $z = 2.5$ cm; (*c*) $t = 102$ μs, $z = 4$ cm.

ring inducer (see figure 1, direction A). The shadow picture sequence of figure 4 is taken during different runs, by varying the time delay of the laser pulse with respect to start-up of the inducer.

The shadow pictures in figure 4 clearly show the discontinuity pattern typical of shock waves undergoing Mach reflection (compare with figure 3). The Mach wave cannot be seen in the first shadow photograph because of inadequate spatial resolution. In accordance with the theoretical curve 1 in figure 5 (see §4), the radius r_m of the Mach disk at this time instant should be less than 0.1 mm, and the Mach

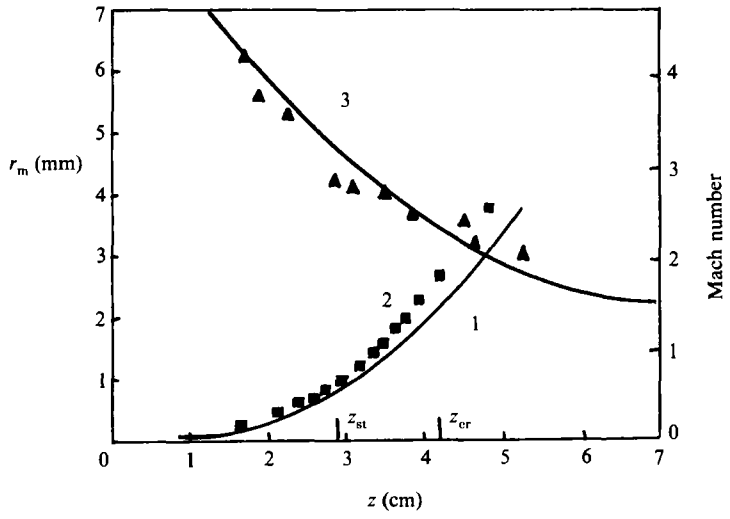

FIGURE 5. Curve 1, Mach wave radius $r_m = f(z_m)$ (theory); squares 2, experimental radius of Mach wave; 3, velocity of Mach shock.

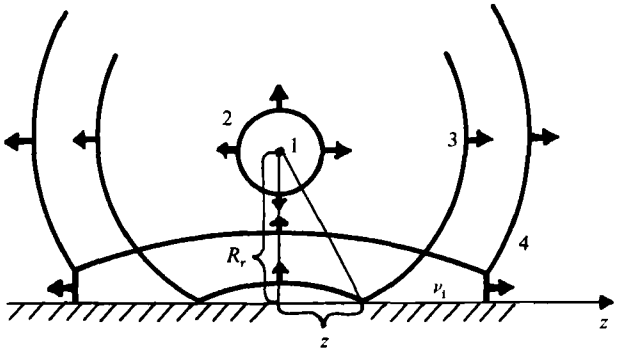

FIGURE 6. Reflection of a spherical shock from a rigid plane. Curve 1, the centre of the blast; 2, expanding spherical shock; 3, regular reflection; 4, Mach reflection.

configuration at such a scale cannot be resolved by means of our shadow technique. Nevertheless a marked distortion of the incident shock front, resulting from acceleration of the ring shock due to amplification, is clearly visible near the axis.

The experimental radius r_m and velocity $M_m = V_m/V_{so}$ of the Mach wave obtained by the use of shadow photographs are given in figure 5. It should be emphasized that we investigated the Mach wave in the range of z-values where its radius is very small ($\leqslant 1$ mm), much less than the characteristic value of the z-coordinate ($\geqslant 1$ cm). So there are different scales for r_m and z in figure 5.

Should the amplification effect be absent, the angle of incidence ν_i would be given by the simple formula

$$\nu_i = \arctan(z/R_r). \tag{3.1}$$

For example, (3.1) would hold in the case of regular reflection of a spherical (or cylindrical) blast wave from a rigid plane (see figure 6). Here we imply that R_r is the height of the centre of the blast, and z is the distance between the projection of the blast centre on the plane and a point where the incident wave intersects the plane.

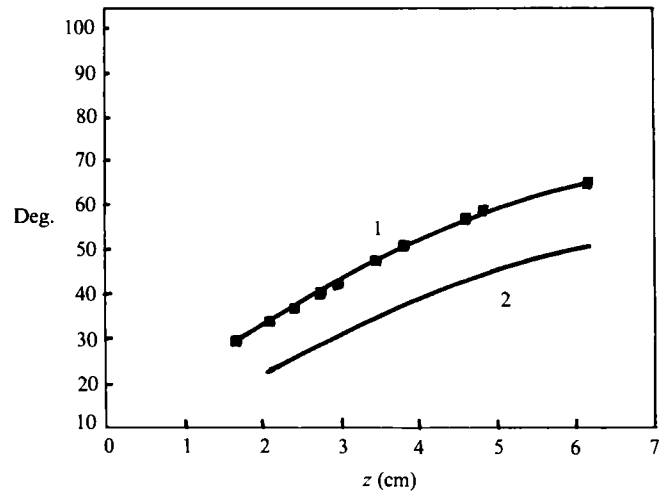

FIGURE 7. Experimental angle of incidence (curve 1), measured at a triple point, compared with the reflection of a spherical shock from a rigid plane (curve 2).

In this case the transition from regular to Mach reflection would be coincident with the point where $\nu_i = \nu_{cr}$, ν_{cr} being the critical angle.

Regular reflection is known to be impossible when the incidence angle exceeds the critical angle ($\nu_i > \nu_{cr}$). In the controversial range of incidence angles $\nu_{st} < \nu_i < \nu_{cr}$, both kinds of reflection are possible. In any event, Mach reflection would be impossible for $\nu_i < \nu_{st}$ (Courant & Friedrichs 1948).

The coordinates z_{cr} and z_{st} that would correspond to $\nu_{cr} \approx 40°$ and $\nu_{st} \approx 30°$ according to (3.1), are shown in figure 5. These values of ν_{cr} and ν_{st} are taken for $M_0 \approx 2.5$ (Bazhenova & Gvozdeva 1977). Our experimental data clearly indicate that a Mach wave exists even at $z < z_{cr}, z_{st}$. This fact displays the effect of amplification upon the reflection of shock waves from the axis.

Moreover, the trend of the $r_m(z)$ curve (see figure 5) is quite consistent with the theoretical statement that the reflection of the wave from the axis of symmetry proceeds in the Mach manner, even at infinitesimal z.

The existence of a Mach wave at small values of z is connected with the increase in the angle ν_i due to the incident wave acceleration near the axis. To illustrate this effect, observed values of the angle of incidence ν_i (measured at the triple point) are presented in figure 7 (curve 1). These values are greater than those calculated using (3.1) (curve 2).

It should be noted that in our case Mach reflection occurs in the 'controversial' range of observed incidence angles $\nu_{st} < \nu_i < \nu_{cr}$.

Another experimental result is a sequence of shadow photographs (see figure 8) obtained by using another direction of the probing laser beam. Namely, the beam is directed along the axis and the plane of the image coincides with the plane of the ring (see figure 1, direction B). The good symmetry of the ring shock wave near the axis confirms the presence of amplification effects at small distances from the axis (figure 5).

A deviation from axial symmetry and the role of shape perturbations of the ring shock front are analysed in Barkhudarov *et al.* (1988).

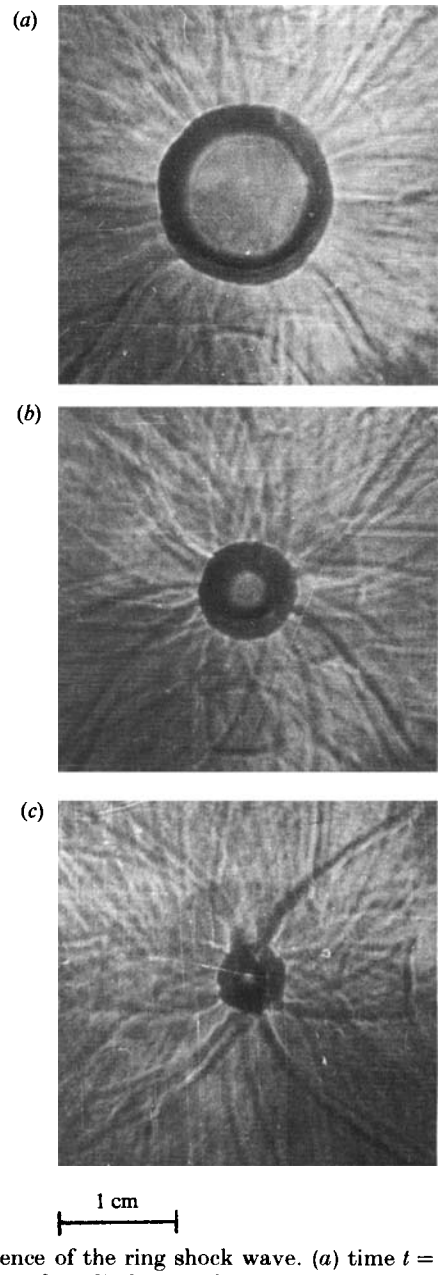

FIGURE 8. The convergence of the ring shock wave. (*a*) time $t = 65$ μs after the beginning of surface discharge; (*b*) $t = 72$ μs; (*c*) $t = 75$ μs.

4. Comparison of the experimental results with the theory

To compare the results of the theory with the experiment it is necessary to use the relation (2.33) between χ and ν_1, because the experimental value of ν_1 is slightly above ν_{st}.

Now we adopt an approximate relation $\chi(\nu_1)$ for $\nu_i > \nu_{st}$. We have already noted that $\chi = 0$ when $\nu_1 = \nu_{st}$, so we can try to use an expression $\chi(\nu_i)$ that tends to zero as $\nu_1 \to \nu_{st}$. For example this could be

$$\chi = 0.33\,(\sin \nu_i \cos^{1/n} \nu_i - \sin \nu_{st} \cos^{1/n} \nu_{st}), \tag{4.1}$$

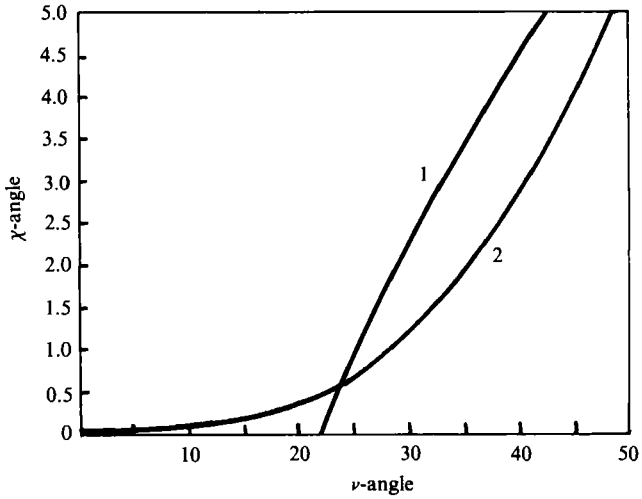

FIGURE 9. The angle of motion of a triple point as a function of the angle of incidence: curve 1 corresponds to the relation (4.1), and curve 2 is obtained from Whitham's theory (Bazhenova & Gvozdeva 1977).

in which $\nu_{st} = 22°$ is the stationary Mach reflection angle for $M \gg 1$. The curve $\chi = f(\nu_i)$ corresponding to (4.1) is shown in figure 9 (curve 1). For comparison the corresponding curve 2, obtained from Whitham's theory (Bazhenova & Gvozdeva 1977), is also presented. The factor 0.33 in (4.1) is selected to give the best agreement with the present experiment.

Combination of (4.1) and (2.34) ($dr_m/dz \sim \chi$) gives the equation

$$dy/dx = 0.33\,(x/y^{1/n} - 0.37). \tag{4.2}$$

Here, $y = r_m/R_0$, $x = z/R_0$. The constant R_0 is estimated from (2.34) by introducing experimental values of the ν_i (figure 7) and the corresponding radius r_m (figure 5). This gives $R_0 \approx 12$ cm. Equation (4.2) is solved numerically. The resulting curve is shown in figure 5 together with the experimental one. The theoretical curve provides an estimate of the radius of the Mach wave for $z < 2$ cm, when experimental observation of it is difficult.

5. Conclusion

The ring shock wave undergoes Mach reflection from the axis of symmetry at small (infinitesimal, according to the theory) values of the axial coordinate z. The observed axisymmetric shock wave reflection pattern results from an increase of incidence angle due to amplification.

The authors thank Drs S. V. Bulanov, I. A. Kossyi and A. A. Savin for helpful discussions and advice.

REFERENCES

BARKHUDAROV, E. M., KOSSYI, I. A., MDIVNISHVILI, M. O., SOKOLOV, I. V. & TAKTAKISHVILI, M. I. 1988 Non-one-dimensional converging shock waves. *Fluid Dyn.* **N2**, 164–170.

BAZHENOVA, T. V. & GVOZDEVA, L. G. 1977 *Non-stationary Interactions of Shock Waves*. Moscow: Nauka (in Russian).

BEREJETSKAYA, N. K., BOLSHAKOV, E. F., GOLUBEV, S. K., DOROFEYUK, A. A., KOSSYI, I. A., SEMENOV, V. E. & TEREKHIN, V. E. 1984 Gas-dynamic phenomena accompanying a ring surface discharge. *Sov. Phys., J. Exp. Theor. Phys.* **87**, 1926–1933.

COURANT, R. & FRIEDRICHS, K. O. 1948 *Supersonic Flows and Shock Waves.* Interscience.

GUDERLEY, G. 1942 Strong spherical or cylindrical shock waves near the centre or the axis (in German). *Luftfahrtforschung* **19**, 302.

KOSSYI, I. A., KRASNOBAEV, K. V., SOKOLOV, I. V. & TEREKHIN, V. E. 1987 Cumulation of shock waves excited by axisymmetric slipping discharge. *Sov. Phys. – Lebedev Inst. Rep.* **N11**, 3–5.

NAYFEH, A. H. 1981 *Introduction tc Perturbation Techniques.* Wiley.

SOKOLOV, I. V. 1986 Behaviour of an axisymmetric shock wave in the neighbourhood of cumulation point. *Sov. Phys., J. Exp. Theor. Phys.* **91**, 1331–1335.

STANYUKOWICH, K. P. 1955 *Non-steady Motions of Continuous Medium.* Moscow: Gostekhizdat (in Russian).

WHITHAM, G. B. 1974 *Linear and Nonlinear Waves.* Wiley.